

A COMPARATIVE STUDY OF PHOTO-CATALYTIC DEGRADATION EFFICIENCY OF METHYLENE BLUE DYE IN WASTE WATER USING POLY(AZOMETHINE)/ZnO NANOCOMPOSITE AND POLY(AZOMETHINE)/TiO₂ NANOCOMPOSITE

S. J.PRADEEBA^a, K. SAMPATH^{b,*}

^a*Department of Chemistry, Hindusthan College of Engineering and Technology, Coimbatore, Tamil Nadu, India.*

^b*Department of Chemistry, Kumaraguru College of Technology, Coimbatore, Tamil Nadu, India.*

**Email id: sampathchemistry@gmail.com*

The poly(azomethine)/ZnO nanocomposites and poly(azomethine)/ TiO₂ nanocomposites were prepared and exemplified by Fourier Transform-Infra red spectroscopy, UV-Visible spectroscopy, Powder X-ray diffraction, EDAX, SEM and TEM techniques. Methylene blue was debased from water using poly(azomethine) (PAZ), titanium di oxide (TiO₂), Zinc oxide, poly(azomethine)/ titanium di oxide (PAZ/ TiO₂) and poly(azomethine)/ titanium di oxide (PAZ/ ZnO) nanocomposites as photo-catalyst in presence of natural sunlight. The deprivation efficiency and reaction kinetics was calculated and the outcome of the photo-catalytic experiments proved that the PAZ/ ZnO and PAZ/ TiO₂ nanocomposites reveals excellent photo-catalytic activity and efficient for achromatize the dyestuff present in the waste water than PAZ, ZnO and TiO₂ in presence of normal sunlight. The maximum degradation efficiency 97% was obtained for PAZ/ ZnO nanocomposite at optimum dosage of catalyst as 500mg and 50ppm of methylene blue dye concentration respectively. The maximum deprivation time was 5hrs. After photo-catalytic study the samples were portrayed by FT-IR and UV-Visible spectroscopy. The main aim of this research was to protect our environment from the contamination of water due to the effluence released from dyestuff industries, to resolve this crisis effective nanocomposite were synthesized.

(Received April 12, 2018; Accepted June 29, 2018)

Keywords: Poly(azomethine), TiO₂, ZnO Photo-catalyst, Nanocomposites, Advanced oxidation process, Degradation efficiency

1. Introduction

Synthetic dyes are poisonous and heavy chemicals that can produce concentrated colors are dangerous to the surroundings. These dyes are opposed to bio-decomposition and have pernicious effect on human health. Adsorption, ultra filtration, extraction, oxidation ozone and hydrogen peroxide are some of the conservative technique utilized to eliminate color from industrial runoff noxious materials [7]. Advanced oxidation processes (AOPs) are substitute to all other techniques, of which the photo-catalysis is the most popular one. In current scenario, heterogeneous photo-catalysis technique can direct to the full deterioration of various inorganic, organic dyes in industrialized operations. There are many semiconductor components are available which acts as photo-catalyst such as TiO₂, MnO₂, ZnO etc. The system depends on the concept of decaying various organic hazardous substances speedily and not a particular one. Among many photo-catalyst element, TiO₂ and ZnO are the best photo-catalyst because they have broad band gap. TiO₂ is the extensively favored because it is harmless, steady, biologically static, excellent absorption / desorption properties, safety and photo corrosion stability [8]. A TiO₂ photo-catalyst has achieved several significant in the ancient times due to its outstanding quality of degrading the

*Corresponding author: sampathchemistry@gmail.com

huge variety of ecological pollutants such as bacteria, organics, viruses and the subsequent discovery of photo activated for water separating of TiO_2 .

Amongst the semiconductors, TiO_2 is the extensively utilised as photo catalyst because of its elevated photocatalytic property, good strength and poison less. ZnO is a good semiconductor material with comparable energy band gap to TiO_2 , reveals an enhanced effectiveness than TiO_2 in photocatalytic deprivation of some pollution and is receiving good attention. Conversely, by virtue of fast rejoining of charge carriers, reaction rate is low in presence of solar radiation and major disadvantage of photocorrosion, the utilization of ZnO is restricted to some extent. In order to overcome these disadvantages, essential attempt has been made to prevent the rejoining of photo generated hole/electron pairs and upgrade the utilization effectiveness of solar radiation in photocatalytic reaction by exterior modification was done such as precious alloy doping or narrow band gap semiconductors combination [35]. The outcome of the photo-catalytic deprivation of biphenyl by TiO_2 with UV light illumination in the year 1976 has created more interest in the ecological application of the TiO_2 as photo-catalyst. Though the band gap of TiO_2 (anatase) is 3.2eV so it can only absorb and be energized by UV illumination with a wavelength below 387nm UV light accounts for <5% of solar illumination. The intrinsic property of anatase limits realistic application. In order to get more efficiency conjugated polymers are used to blend with these semiconductor materials.

Conjugative polymer / TiO_2 hybrid stuff reveals more effectiveness in deterioration of organic contaminants in presence of both UV light and visible illumination. By means of this blending technique, it was found to be complicated to attain electric contact among the metal oxide particles and the conjugative polymer layer, because the polymer chain might hinder with the correlation produced inside the metal oxide. Entire hybridization might not be achieved using the diffusion technique as the polymer may not be filled because of the inadequate penetration power of the conductive polymer film. Since the conjugative polymers merely placed on the TiO_2 and ZnO nanoparticles, but the boundary linking the TiO_2 and ZnO semiconductor and the conjugative polymer layer does not balance. A steady border for the hetero function composite is extremely advantageous since it promotes the speed of charge injection when accelerates by light or electrical motivation. UV accelerates the TiO_2 produce conduction band electrons (e^-) and valence band holes (h^+) in couples provide surface –mediated reduction-oxidation activities.

Now- a-days, there is rising interest in using polythiophenes, polyaniline, polypyrrole and their derivatives to sensitive TiO_2 produce polymer/ TiO_2 nanocomposites. Like this several nanocomposites such as polypyrrole/ TiO_2 composite particles polythiophene/ TiO_2 composite particles, polyaniline / TiO_2 composite particle, poly (3-hexyl thiophene) / TiO_2 nanocomposite were also prepared and its effective deprivation of dye stuffs like methyl orange, methylene blue, rhodamine -B under UV and visible sunlight have been recorded in the past decades [1-15].

Among the various dyestuffs discharge from textile industries, methylene blue pollute the environment more and it affects the aesthetic appearance of environment. The IUPAC name of methylene blue was [7-(dimethylamino)phenothiazin-3-ylidene]-dimethylazanium;chloride. It is used for textile, paper, food additives and leather industries and it is a heterocyclic organic dye. It is an odourless, dark green solid powder which gives a navy blue solution when it is dispersed in water and it is a really destructive chemical that is mainly used as a dye. Higher concentration of dye effluents discharge in to water leads to discomfort in aquatic organisms, it changes the ecosystem and ill effects like tissue necrosis, vomiting, jaundice, cyanosis and diarrhea which is the main reason of degradation of methylene blue. So in the present study was based on the removal of methylene using polymer nanocomposite material.

By analyzing the previous studies, there have been no reports on nanocompounds of poly (azomethine) PAZ / TiO_2 and ZnO as a photo-catalyst. So conjugative polymer poly(azomethines) are used to make composite with TiO_2 and ZnO to acts as photo-catalyst. Moreover, the poly(azomethines) present the advantages to be p- and n-doped, due to their reversible oxidation and reduction, correspondingly [41]. Conjugated poly(azomethines) (PAZ), polyamines or poly (Schiff bases) are an additional fascinating class of conjugative polymers holding nitrogen atom ($\text{CH}=\text{N}$) in a polymer backbone is used in this study for producing nanocomposites along with TiO_2 .

Based on the above concept, in this article, poly(azomethine) PAZ, TiO₂, ZnO, PAZ/TiO₂(PNT), PAZ/ZnO(PNZ)nanocomposites were prepared and structural characterization such as FT-IR, UV-Vis, SEM, TEM, XRD and EDAX were conferred. The photocatalytic experiments with poly(azomethine) PAZ/ TiO₂andPAZ/ZnOnanocomposites were examined for the removal of methylene blue present in waste water was carried out in presence natural sunlight. Deprivation efficiency of photocatalyst such as poly(azomethine) PAZ/ TiO₂ and PAZ/ZnO nanocomposites were evaluated.

2. Materials and methods

2.1. Reagents and materials

Highly uncontaminated chemicals were purchased from Sigma Aldrich, they are p-phenylene diamine (99.98), Hexamethylenetetramine (99.98), ethanol(99.98), 4,4'-bis (chloro methyl) biphenyl (99.98), toluene, DMF(99.98), methanol (99.98), titanium tetra chloride, ammonium hydroxide, Zinc nitrate, potassium hydroxide and methylene blue.

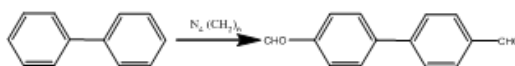
2.2 Experiments

Preparation of poly(azomethine)

Monomer Preparation

Synthesis of 4,4'-diformyl biphenyl

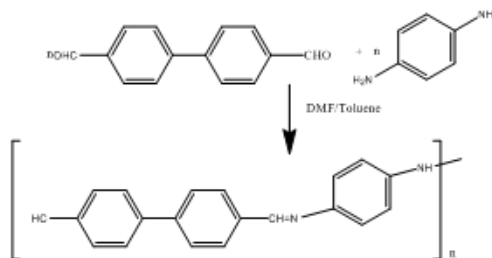
Hexamethylenetetramine (6.8, 48mmol) was dissolved in ethanol (90 ml) and 4,4'-bis (chloro methyl) biphenyl (3.00gm, 12mmol) was added at 400C. The combination was stirred 1.5hr at 45-50⁰C and precipitate was collected, washed with ethanol for two times. Then acetic acid (40ml) 50% was added. Reflux the substance for 10 hrs and filtrated. The filtrate was cooled overnight. The crystals (Scheme-1) were accomplished.



Scheme 1- Synthesis of 4,4'-diformyl biphenyl

Synthesis of poly(azomethine)

In a 25ml of RB flask with a magnetic stirrer a condenser and inlet –outlet dean stark system 0.1536 g (0.5mmol) of 4,4'-diformyl biphenyl and 0.05456g (0.5mmol) of p-phenylene diamine, 7ml of DMF and 2 ml of toluene were introduced. The reaction mixture was refluxed at the boiling temperature of toluene for 6 hrs. After cooling at room temperature the reaction mixture was added in a huge amount of methanol and the polymer precipitate (Scheme-2) was filtered and dried.



Scheme 2 –Synthesis of Polyazomethine

Synthesis of Nano ZnO

In this work, the aqueous solution (0.2M) of Zinc nitrate and the solution (0.4M) of KOH were prepared with distilled water respectively. The KOH solution gradually poured in to zinc nitrate solution at room temperature under strong stirring, which resulted in the development of a white suspension. The white suspension was washed 3 times with distilled water and centrifuged and washed with absolute alcohol at last. The gained product was calcined at 500°C in air atmosphere for 3 hrs.

Synthesis of Nano TiO₂

TiCl₄ was slowly introduced into de-ionised double distilled water in an ice bath (0°C) under constant stirring until it was completely dissolved and then 18ml of 30% ammonium hydroxide was added to this suspension. The formed white titanium hydroxide was allowed to stand for 1hr. Then, the obtained TiO₂ nanoparticles were filtered, washed with deionised double distilled water and dried at 100°C in a vacuum oven for 3hr [14].

Preparation of making polymer nanocomposite

Only a small amount of polymers were taken to prepare the composites. The polymer (250mg) was dissolved in 100ml DMF by stirring in 250ml Stoppard conical flask kept in a shaker and sonicated to obtain a dispersed polymer solution. The polymers were incompletely soluble in DMF and continued finely dispersed after 48hr. The relevant nanoparticles dispersed in acetone were sonicated and instantaneously added to the polymer in DMF under sonication. The polymers were permitted to precipitate out. While precipitating, the nanoparticles got encapsulated in to the polymer matrix. The composites thus acquired were filtered and washed systematically with acetone and dried [36].

2.3 Characterization

FT-IR spectroscopy (BRUKER EQUINOX-55), UV-Vis spectroscopy (SHIMADZU), Powder X-ray Diffraction (Scintag-XDS-2000 meter), Scanning Electron microscope (JSM-7600F Japan), Transmission Electron Microscopy TEM (JEOL model 2100) and EDAX of the sample were recorded for structural characterization.

2.4 Photocatalytic experiments

The photo catalytic activities of PAZ, PAZ/TiO₂ and PAZ/ZnO nanocomposites were performed using methylene blue dyes in presence of natural sunlight. Before irradiation the suspension was mixed magnetically for 30 minutes in absence of light until adsorption-desorption equilibrium was recognized and then suspension were illuminated by light source with stirring. Dye stock solution was produced by 4mg of dye is soluble in 500ml of DI water. The different amount of catalyst (PAZ, PAZ/TiO₂ and PAZ/ZnO) was added to remove methylene blue and kept in natural sunlight. Initial and final concentrations of dye solution were measured by recording absorbance on a double beam UV-Vis spectrophotometer at 516nm respectively. The samples were received at different time period and concentration of the dye was calculated using UV-Vis spectroscopy. The photo degradation efficiency R (%) was calculated by the employing the following equation

$$R (\%) = \frac{C_0 - C_t}{C_0}$$

where C₀ symbolize the concentration of dye before irradiation and C_t denotes the concentration of the dye after a definite illumination time respectively [15-19].

3. Results and discussion

3.1 Characterization of Photocatalyst

3.1.1 Fourier transform-Infra red spectroscopy

A representative FT-IR spectrum of PAZ, TiO₂, ZnO, PNT, PNZ, PAZMB, PNTMB and PNZMB are reproduced in (Fig-1 a, b, & c). The characteristic band of azomethine or imine linkage (-CH=N) appeared at 1512 cm⁻¹. The absorption band at about 3736 cm⁻¹ is related with the N-H stretching vibration in the aromatic unit. The absorption spectra at 3555 cm⁻¹ is attributed to the C-H stretching in aromatics. The peaks at 1387 and 1352 cm⁻¹ are endorsed to C=C stretching in benzene ring. The peaks visible at 809 cm⁻¹, 811 cm⁻¹, 872 cm⁻¹ are the region for N-H stretching vibration respectively. The absorption peak at 464 cm⁻¹ belongs to the ZnO nanoparticle and the same peak was observed in PAZ/ZnO (PNZ) composite but not seen in PAZ spectrum. The absorption peak at 800 cm⁻¹ corresponds to the Ti-O-Ti stretching mode [15] and the same peak was observed in PAZ/ TiO₂ (PNT) composite but the intensity of that peak is not observed in PAZ spectrum.

The PAZ/ZnO (PNZ) nanocomposites exhibits similar characteristics peaks like PAZ (Fig-1b). The minor alteration in high peak magnitude and wavenumbers may be the outcome of the interaction with PAZ chains and ZnO particles [20-25]. The PAZ/ TiO₂ (PNT) nanocomposites displays related distinctive peaks like PAZ, moreover it shows the quality absorption of Ti-O-Ti at about 800 cm⁻¹ (Fig-1b). Slight alteration in high peak magnitude and wave numbers may be the outcome of the interaction with PAZ chains and TiO₂ particles [20-25].

After the photocatalytic process respective FT-IR spectrum of PAZ and PAZ/ZnO (PNZ), PAZ/ TiO₂ (PNT) were observed (Fig-1c). The peaks are similar for PAZ only and slight variation due to absorption of methylene blue (PAZMB) dye. In case of PAZ/ZnO (PNZ) and PAZ/ TiO₂ (PNT) the peaks remains same position like PAZ but the intensity of peaks have been reduced, it shows the degradation efficiency of methylene blue (PNTMB, PNZMB) than PAZMB.

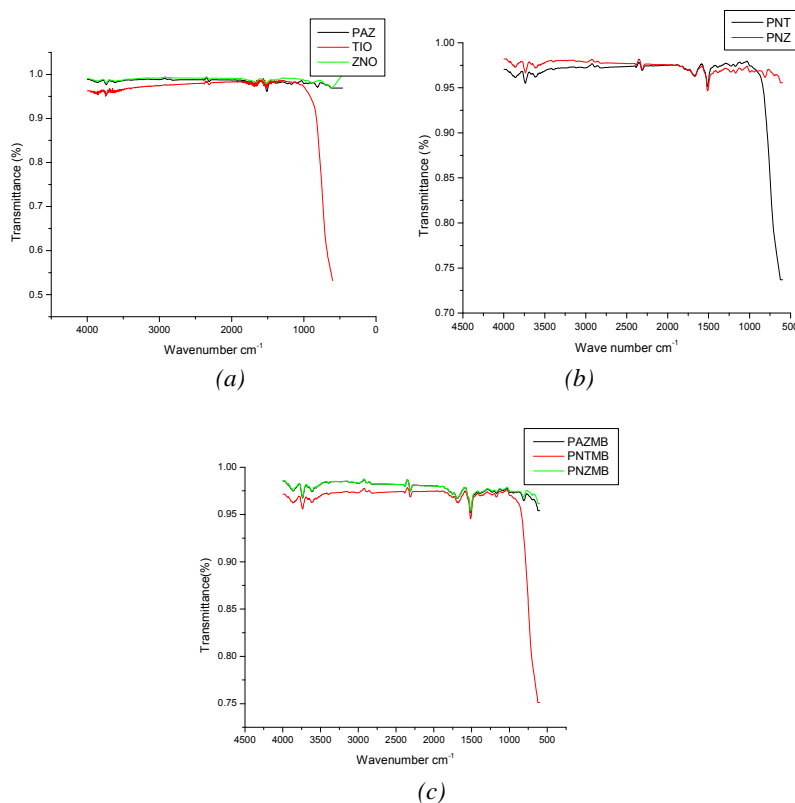


Fig. 1. FT-IR characterization of PAZ, TiO₂ & ZnO (a), PNT & PNZ (b) and after removal of methylene blue using PAZ, PNT & PNZ are PAZMB, PNTMB & PNZMB (c).

UV-Visible Spectroscopy

The UV-Vis spectrum (Fig. 2a,b & c) displays the absorption band in the series of 280-290nm was designated to the π - π^* and n- π^* transition in the conjugated chain present in the structure of TiO₂, ZnO, PAZ/TiO₂ and PAZ/ZnO nanocomposites. The absorption range of the ZnO nanoparticles (Fig. 2a) shows a sharp absorption peak around 378 nm which is the typical single peak of hexagonal ZnO particle. It indicates the UV spectrum might create excitation of electrons present in the lower energy level of ZnO to the higher energy level i.e. valence band to conduction band. The peak in the range of 378 nm is present in ZnO and PAZ/ZnO (PNZ) nanocomposites but not observed in PAZ (Fig. 2a). Therefore the prepared can be photo stimulated by visible light or existing natural sunlight illumination which has no destructive effect on human health [26-30]. Similarly TiO₂ has shown strong absorption at 296 nm when TiO₂ nanoparticles were incorporated into the polymer matrix, a slight shift in the absorption band of TiO₂ from 296 nm to 300 nm was observed which indicated the formation of PAZ/ TiO₂ (PNT) nanocomposite (Fig-2a). Sudden change in the absorption peak at around 350 nm to 390 nm is due to the electron transition from the valence band to the conduction band [12]. The peak in the range of 296 nm is present in TiO₂ and PAZ/ TiO₂ (PNT) nanocomposites but not observed in PAZ (fig-2a). It was noticed that peak intensity was higher for the entire three spectrums (fig-2a) it shows hyperchromic effect which indicated presence of auxochrome group like -NH₂ & -O in the structure. Therefore the prepared nanocomposite can be photo stimulated by visible light or existing natural sunlight illumination which has no destructive effect on human health [26-30].

After the photocatalytic process respective UV-Vis spectrum of PAZ and PAZ/ZnO were observed (Fig. 2c). The appearance of absorption band in the range 500-700 nm PAZ/ZnO (PNZ) nanocomposites is due to the colour absorption of methylene blue (PNZMB) present in water. But, absorption band in the range of 500-700 nm was not observed in PAZ (Fig-2b) it shows the dye removal of methylene blue (PAZMB) is less when compared to PAZ/ZnO (PNZ) and PAZ/ TiO₂ (PNT) nanocomposites (Fig. 2c).

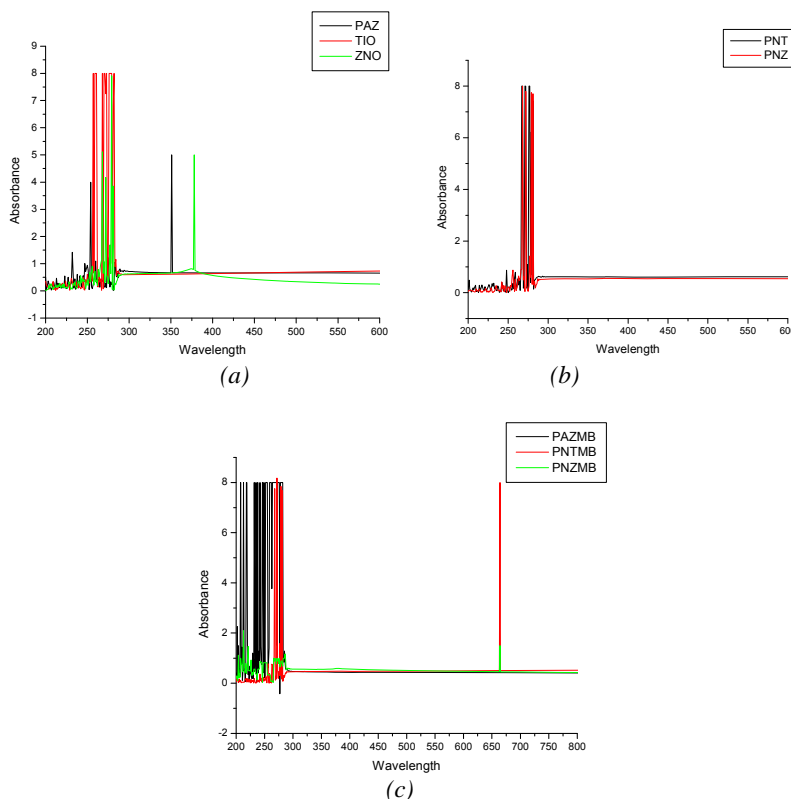


Fig. 2. UV-VIS characterization of PAZ, TiO₂&ZnO (a), PNT & PNZ (b) and after removal of methylene blue using PAZ, PNT & PNZ are PAZMB, PNTMB & PNZMB (c).

X-Ray diffraction

Figs. 3-7 shows the XRD pattern of PAZ, ZnO, TiO₂/PAZ/ZnO and PAZ/ TiO₂. Generally polymers exhibited a broad halo in the wide angle region (at about $2\theta=20^\circ$) indicating that the polymers were amorphous. The peak at $2\theta=20^\circ$ also symbolizes the characteristics interval linking the ring planes of aromatic units in neighboring chains or the convenient association with inter-chain distance. Further, the sharp peak centered at $2\theta=25^\circ$ might be consigned to the spreading from PAZ chains at inter planar interval distance and specify the PAZ had also same degree of crystalline [36].

In the XRD model of ZnO the peaks at $2\theta=31.76, 34.4, 36.2, 47.53, 56.60, 62.86, 66.37, 67.96, 69.09$ appear which are ascribed to be (100), (002), (101), (102), (110), (103), (200), (112) and (201) correspondingly. This indicated that the ZnO element acquire a hexagonal crystal structure (JCPDS No 36-1451). In figure 4&5 the major diffraction peaks of PAZ/ZnO composites are parallel to those of clean ZnO particles. This concludes that the PAZ placed on the exterior of ZnO particles and the crystalline structure of ZnO was not influenced by the alteration of poly(azomethine) PAZ. Therefore, the XRD patterns of composites propose a flourishing merging of nano-ZnO in PAZ composites [40].

The XRD pattern of TiO₂ shows diffraction peaks at 2θ values of 25.53, 38.34, 48.38, 54.61, 55.64, 63.21, 69.21, 69.14, 75.42 corresponding to the (101), (004), (200), (105), (211), (204), (116) and (215) which could be attributed to the anatase phase in the TiO₂ (JCPDS-87-0598).[14] In figure 5&6 the major diffraction peaks of PAZ/TiO₂ composites are parallel to those of clean TiO₂ particles. This concludes that the PAZ placed on the exterior of TiO₂ particles and the crystalline structure of TiO₂ was not influenced by the alteration of poly(azomethine) PAZ. The addition of PAZ species did not change the crystalline phases of TiO₂. However the intensity of the peaks of TiO₂ is lower in the case of PAZ/ TiO₂ nanocomposite than that of nano TiO₂ suggesting that theTiO₂ particles are uniformly embedded in the polymer matrix of PAZ/ TiO₂. Therefore, the XRD patterns of composites propose a flourishing merging of nano- TiO₂ in PAZ composites [40].

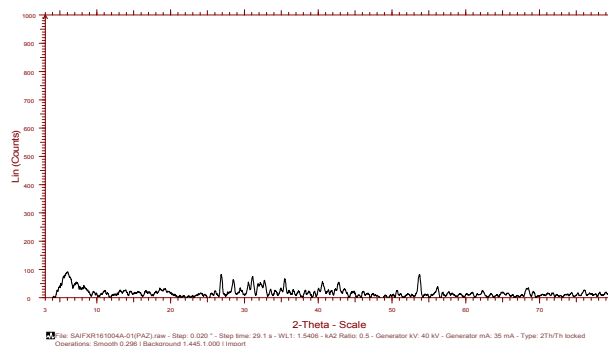


Fig. 3. XRD of Poly(azomethine).

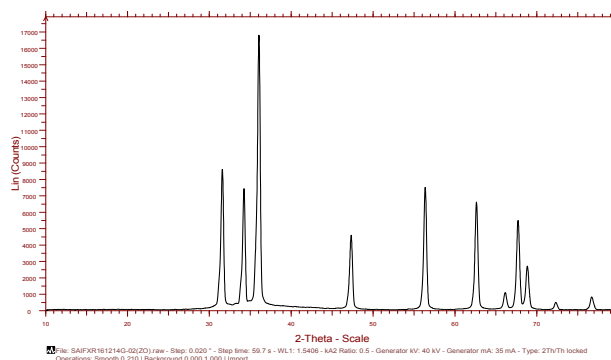


Fig. 4. XRD of ZnO.

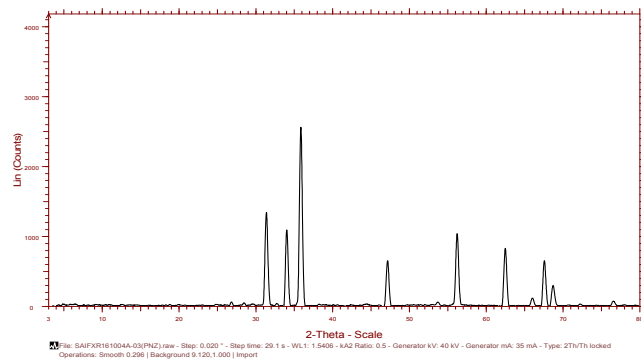


Fig. 5. XRD of Poly(azomethine)/ZnO.

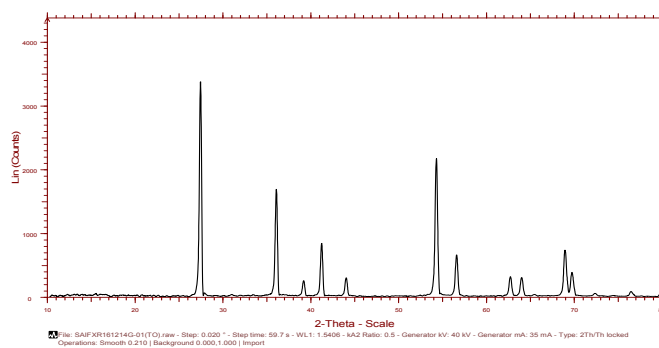


Fig. 6. XRD of TiO₂.

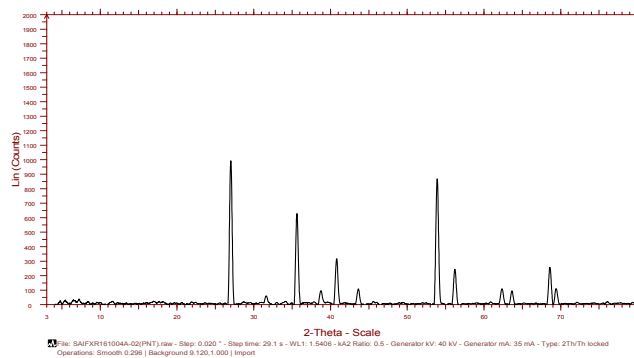


Fig. 7. XRD of Poly(azomethine)/TiO₂.

Morphological studies

The SEM image of ZnO nanoparticles (Fig. 8c) with a diameter of nearly 10 nm and a crystalline structure confirm the SEM images of PAZ/ZnO nanocomposite (Fig. 8b) with low and high exaggeration images respectively. Surface modifications of ZnO (Fig. 8c) particles by poly(azomethine) PAZ (Fig. 8a) chain show slight change in the morphology of PAZ/ZnO nanocomposite (Fig. 8b).

The EDAX spectrum (Fig. 8d) prove the presence of Zn and O in the catalyst PAZ/ZnO nanocomposite.

The structural modification of ZnO, poly(azomethine)PAZ and PAZ/ZnO nanocomposites were analysed by TEM method and the outcomes are exhibited in (fig-9). As shown in the figure-9c, it is obviously seen that the precise ZnO in a combination of ellipsoidal nanoparticles of normal dimension around 35nm. The morphology of the composites is related to that of precise ZnO (fig-9 e,f). However the constituent part in the composites tends to aggregate and lump tightly than precise ZnO. This might be owing to the PAZ (fig-9a,b) chains performing as folder in the composite, which hold together or lump the composite particle together. A same outcome was found in another research article [36].

The selected area electron diffraction (SAED) pattern of PAZ, PAZ/ZnO and ZnO (Fig. 9b,d & f) also confirms the binding of composites material together[36].

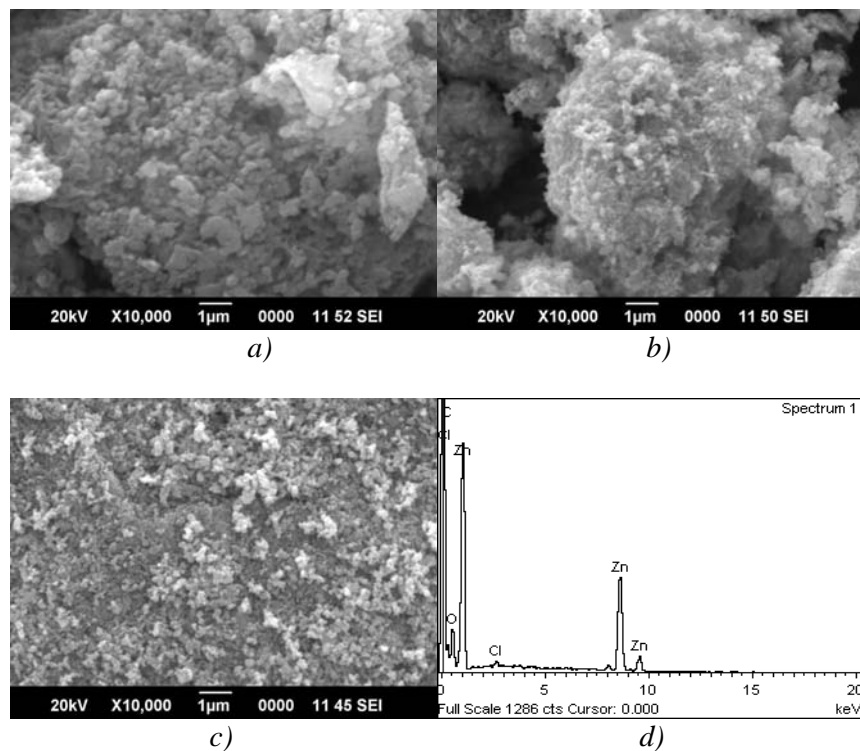


Fig. 8 SEM of PAZ(a), PAZ/ZnO nanocomposite (b) & ZnO (c) and EDAX of PAZ/ZnO nanocomposite (d).

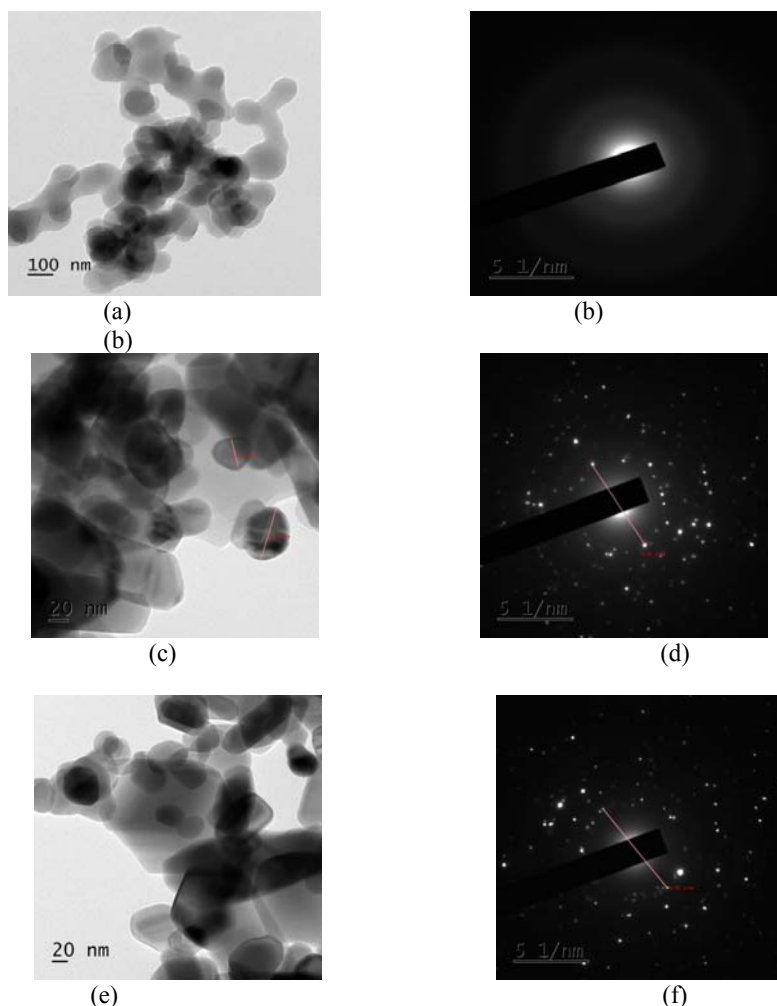


Fig. 9. TEM of PAZ(a,b), PAZ/ZnO nanocomposite (c,d) & ZnO (e,f).

The SEM image of TiO₂ nanoparticles (fig-10c) with a diameter of nearly 10 nm and a crystalline structure confirm the SEM images of PAZ/ TiO₂ nanocomposite (Fig-10b) with low and high exaggeration images correspondingly. Surface alteration of TiO₂ (fig-10c) particles by poly(azomethine) PAZ (fig-10a) chain show minor change in the morphology of PAZ/ TiO₂ nanocomposite (fig-10b).

The EDAX spectrum (Fig. 10 d) proves the presence of Ti and O in the catalyst PAZ/ TiO₂ nanocomposite.

The structural modification of TiO₂, poly(azomethine)PAZ and PAZ/TiO₂ nanocomposites were exemplified by TEM method and the outcomes are exhibited in Fig. 11. As shown in the Fig. 11a-f the nature of the TEM images revealed that all nanoparticles are spherical in shape with uniform structure. The morphology of the composites is related to that of precise TiO₂ (Fig. 11 e,f). However the constituent part in the composites tends to aggregate and lump tightly than precise TiO₂. This might be owing to the PAZ (Fig. 11a,b) chains performing as folder in the composite, which hold together or lump the composite particle together. A same outcome was found in another research article [36]. Moreover, the TiO₂ particles (dark shaded nanoparticle) are determined that they get captured in polymer (light shaded) matrix. These outcomes expose that the TiO₂ particles are not merely mixed up or merged with the polymer, signifying that the TiO₂ particles are implanted in the polymer matrix, which is fairly in conformity with the outcomes of the XRD analysis [11].

The selected area electron diffraction (SAED) pattern of PAZ/ TiO₂ and TiO₂ (Fig-11a,c & f) also confirms the binding of composites material together[36].

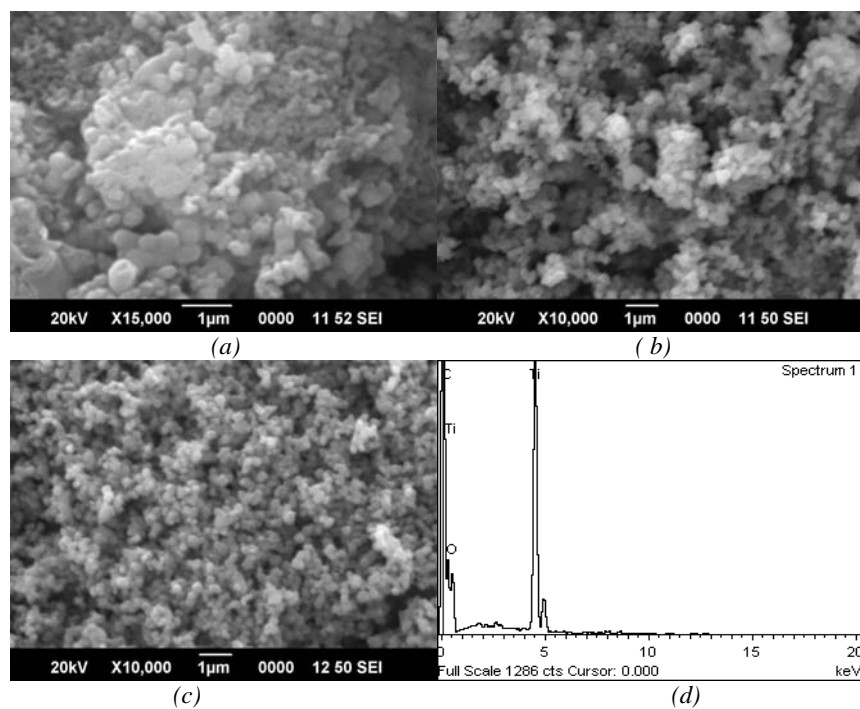


Fig. 10. SEM of PAZ(a), PAZ/TiO₂ nanocomposite (b) & TiO₂ (c) and EDAX of PAZ/TiO₂ nanocomposite (d).

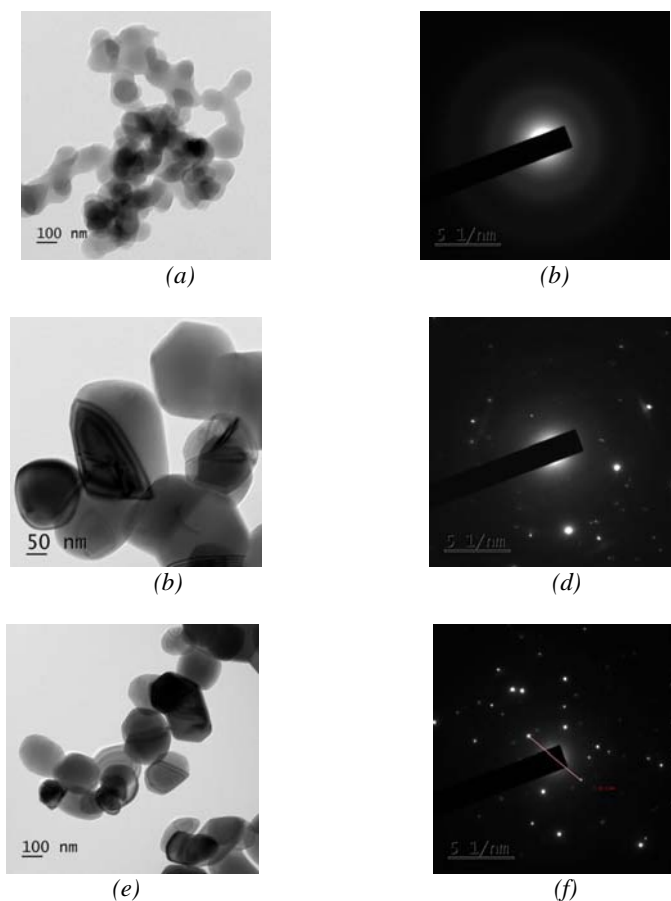


Fig. 11. TEM of PAZ(a,b), PAZ/ TiO₂ nanocomposite (c,d) & TiO₂ (e,f).

Photo catalytic behavior of PAZ/ZnO nanocomposites and PAZ/TiO₂ nanocomposites in presence of natural sunlight

The photo catalytic decomposition of methylene blue using poly(azomethine) PAZ, ZnO, TiO₂, PAZ/ZnO (PNZ) and PAZ/ TiO₂ (PNT) as a catalyst under sunlight irradiation were investigated. By varying the dosage of photocatalyst such as 100,200,300,400 and 500mg at different time intervals (1-5hrs) are shown in the figures 12-16 at constant concentration (50ppm) of dye.

The maximum removal of Methylene blue (97%) dye in water is achieved at 500mg of PAZ/ZnO (PNZ) at 50ppm of dye concentration under natural sunlight radiation in the duration of 5hrs are shown in Table-1. The variation of decomposition vs irradiation time of methylene blue (Fig. 12-16) dye solutions are represented.

The maximum removal of Methylene blue (97%) dye in water is achieved at 500mg of PAZ/ZnO (PNZ) at 50ppm of dye concentration under natural sunlight radiation in the duration of 5hrs than PAZ/TiO₂ (PNT) at 50ppm of dye.

Table.1. Maximum degradation efficiency at 500mg catalyst dosage and 50ppm dye concentration.

Dye Catalyst	Degradation Efficiency (%) of Methylene blue dye
PAZ	86
PAZ/ZnO (PNZ)	97
PAZ/ TiO ₂ (PNT)	95
ZnO	90
TiO ₂	93

The rate constants of photo catalytic decomposition of Methylene blue (MB) dye was determined (C_t/C_0 vs Time fig 12-16) using the following equation [10-13]:

$$\ln C_t / C_0 = K_{app} t$$

$K_{App}(\text{min}^{-1})$ is the pseudo first order kinetics of rate constants. The rate constant for photo catalytic decomposition of methylene blue (MB) was found to be $k=0.2803 \text{ min}^{-1}$.

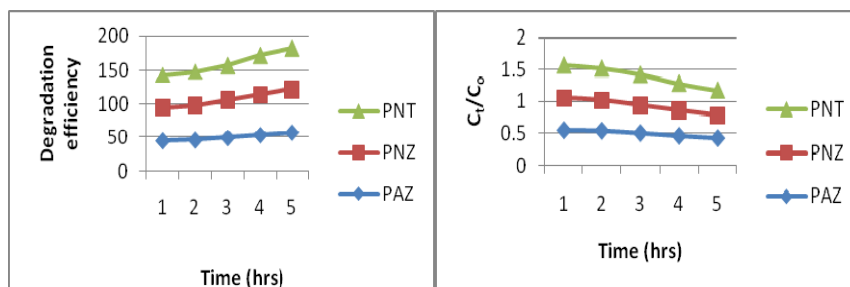


Fig. 12. The result of degradation efficiency and kinetics of MB solution at normal sunlight irradiation using 100mg catalyst PAZ, PAZ/ZnO (PNZ), and PAZ/ TiO₂ (PNT) at 50 ppm dye concentration.

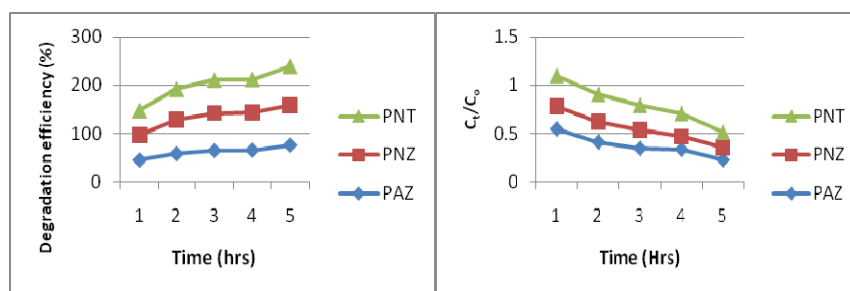


Fig. 13. The result of degradation efficiency and kinetics of MB solution at normal sunlight irradiation using 200mg catalyst PAZ, PAZ/ZnO (PNZ), and PAZ/ TiO₂ (PNT) at 50 ppm dye concentration.

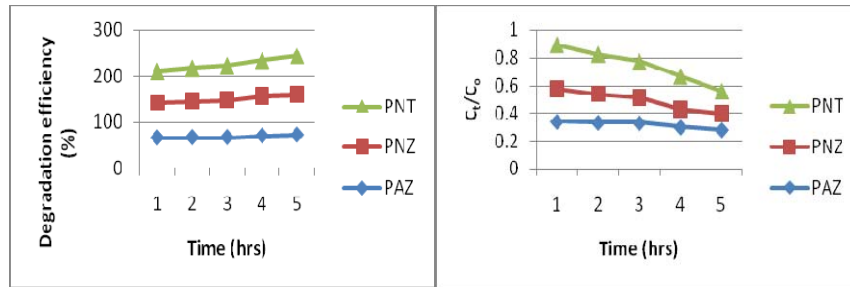


Fig. 14. The result of degradation efficiency and kinetics of MB solution at normal sunlight irradiation using 300mg catalyst PAZ, PAZ/ZnO (PNZ), and PAZ/ TiO₂ (PNT) at 50 ppm dye concentration.

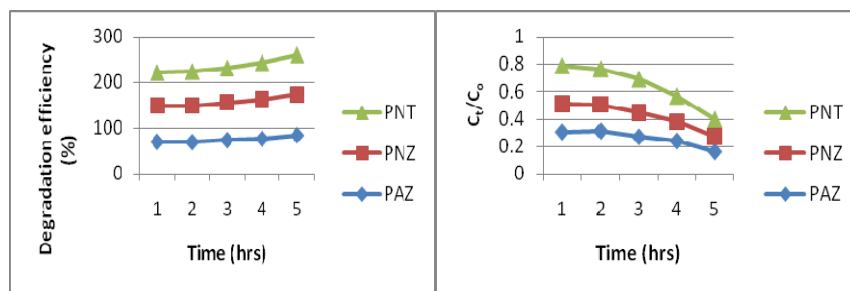


Fig. 15. The result of degradation efficiency and kinetics of MB solution at normal sunlight irradiation using 400mg catalyst PAZ, PAZ/ZnO (PNZ), and PAZ/ TiO₂ (PNT) at 50 ppm dye concentration.

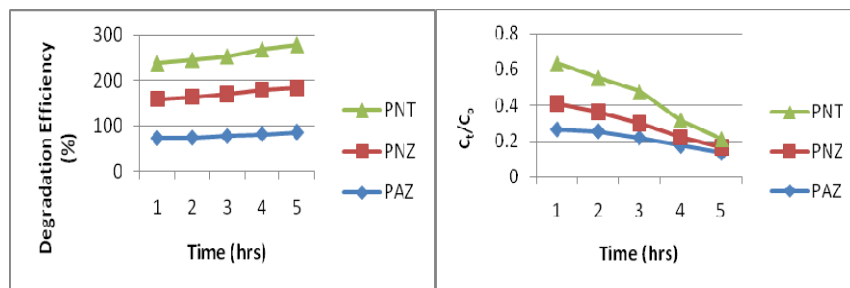


Fig. 16. The result of degradation efficiency and kinetics of MB solution at normal sunlight irradiation using 500mg catalyst PAZ, PAZ/ZnO (PNZ), and PAZ/ TiO₂ (PNT) at 50 ppm dye concentration.

3.2 Mechanism of photo-catalytic activity

In a normal semiconductor photo-catalytic design, electrons of the photo catalyst are energized from the valence band lower energy level to the conduction band higher energy level by the absorbing illumination, an electron energy level conversion happens which directs to the creation of electron - hole pairs. At this point, 2 divergent passages are produced: the created electron hole (h⁺) influencing with another particle is able to be utilized for oxidation reactions and the energized electrons (e⁻) are able to contribute for reduction reactions (Fig. 17).

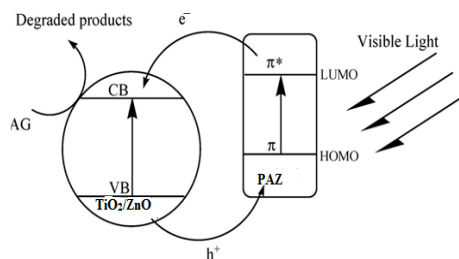


Fig. 17. Schematic Representation of Mechanism of Photo-catalytic reaction of PAZ/TiO₂ and ZnO nanocomposites.

A conjugated structure consists of linked π -orbitals by means of delocalized electrons are responsible for absorbing radiation from sunlight. Because of this, conjugated polymers are large organic molecules their structures are described as different single and multiple bonds with overlapping π -orbitals in their back bone which leads to delocalization. Numerous resources such as PEDOT, polyaniline and polypyrrole have been examined as possible visible light active photo-catalysts. Recently, clean detectable luminous active conjugated polymer photo catalysts have been established, including polyazomethines and polyphenylenes were communicated for H₂ evolution, however the polymer materials were typically energetic in presence of UV-Visible radiation with moderate study [36].

4. Conclusions

In this study, the photocatalytic removal of the dye pollution from the waste water from textile industries by PAZ/ZnO and PAZ/TiO₂ nanocomposites were investigated. The consequence of different parameters such as the dosage variation of photocatalyst, reaction time was tested. The decolorisation times was decreased by increasing the amount of PAZ/ZnO and PAZ/TiO₂ nanocomposites in the range of the tested value 0.500g was the optimum of PAZ/ZnO and PAZ/TiO₂ nanocomposites in the empirical tests conducted in 50ppm of methylene blue dye concentration. The optimum time of the tests in those dosage variations of PAZ/ZnO and PAZ/TiO₂ nanocomposites nanocomposites was 5hrs. It was found that PAZ/ZnO nanocomposite was more efficient photocatalyst than PAZ/TiO₂ nanocomposite in removing methylene blue dye present in waste water.

This protocol may be employed effectively in the treatment of textile dye effluents which are hazardous to the environment, as this synthesized photocatalyst is economically feasible compared to other oxidative process. The present study demonstrates that the synthesized PAZ/ZnO and PAZ/TiO₂ nanocomposites nanocomposites could be used as efficient photocatalyst using the natural sunlight which contributes towards the remediation of pollution.

Acknowledgements

The authors thank the management and principal of Hindusthan college of Engineering and Technology to carry out the work in a successful manner.

References

- [1] Zhu Hua-Yue, Jiang Ru, Guan Yu-jiang, Fu Yong-Qian, Xiao Ling, Zeng Guang-Ming, Separation and purification technology **74**, 187 (2010).
- [2] H.Gopalappa, K.Yogendra, K.M.Mahadevan, N.Madhusydhana, International journal of science research **1**(2), 91 (2012).

- [3] P.Govindhan, C.Pragathiswaran, J.Material science: Mater .Electron 60 (2016).
- [4] H. Al-Kandari, A.M.Abdullah, A. M. Mohammed, S.Al-Kandari, J. Mater.Sci. 74 (2016).
- [5] Sumita Rani, Meenal Aggarwal, Mukesh Kumar, Sumit Sharma, Dinesh Kumar, Water Sci. 98 (2016).
- [6] SamadSabbaghi, FatemeDoraghi,J.Water Environ.Nanotechnol.1(1), 27 (2016).
- [7] Deyong Wu, Fei Wang, Yuanbin, Caolong Li, RSC Adv.6, 73522 (2016).
- [8] Vorrada Loryuenyong, Jaruwancharoensuk, RachayaCharupongtawitch, Amita Usakulwattana, Achanai Buasri, J.Nanosci.Nanotechnol.16, 296 (2016).
- [9] Syed Shahabuddin, Norazilawati Muhamad Sariah, Sharifah Mohamad, Juan Joon Ching, Polymers8, 27(2016).
- [10] F.Petronella, A.Truppi, C.Ingrosso, T.Placido, M.Striccoli, M.L. Curri, A.Agostino, R.Comparelli, Catalysis today16, (2016)
- [11] Bingcai Pan, Yingamai Xie, Shujuan Zhang, Lu Lv, Weiming Zhang, Applied materials & interfaces, 120 (2012).
- [12] M.Mzoughi, William W.Anku, Samuel O.B.Oppong, Sudheesh K.Shukla, EricS.Agorku, Penny P.Govender, Advanced materials letters7(12), 946 (2016).
- [13] Haile Hassena, Modern chemistry and applications 4(1), (2016).
- [14] Xiaosong Zhou, Bei Jin, Jin Luo, Xuyao Xu, LinglingZhang, Jiajia Li, Haojian Guan, RSC Advances6, 64446 (2016).
- [15] Deepak Pathanaia, Divya Gupta, Ala H. Al-Muhtaseb, Gaurav Sharma, Amit Kumar, Mu.Nausad, Tansir Ahamed, Saad M.Alshehri, Jr of photochemistry and photobiology A: Chemistry329,61 (2016).
- [16] Saravanan Rajendran, Mohammad Mansoob Khan, F.Gracia, Jiaqisn Qin, Vinod Kumar Gupta, Stephen Arumainathan ,Scientific research5, 31641 (2016).
- [17] Ruxangul Jamal, Yakupjan Osman,Adalet Rahman, Ahmat Ali, Yu Zhang, TursunAbdiyim , Materials 7, 3786 (2014).
- [18] TursunAbdiriyum, Anmat Ali, Ruxangul Jamal, Yakupjan Osman, Yu Zhang, Nano research letters9, 89 (2014).
- [19] Madhusudhana, Yogendra, Mahadevan, Suneel Naik,International Jr of chemical Engg and application2(4), 294 (2011).
- [20] NarayanappaMadhusudhaa, Kambalagere Yogendra, Kittappa M.Mahadevan, Research Jr of chemical sciences2(5), 72 (2012).
- [21] Thou-Jen Whang, Mu-Tao Hsieh, Huang-Han Chen, Applied surface science258, 2796 (2012).
- [22] RahimehNosrati, Ali Olad, RoyaMaramifar, Environ.Sci. Pollution Research 19, 2291 (2012).
- [23] Yunfeng Zhu, Yi Dan, Solar Energy materials and solar cells 94, 1658 (2010).
- [24] VolkanEskizeybek, Fahriye Sari, Handan Gulce, Ahmet Gulce, Ahmet Avci, Applied catalysis B: Environmental119, 197 (2012).
- [25] Bilge Ozbay, NevimGenc, Ismail Ozbay, Baha Baghaki, Sibel Zor, Clean Techn. Environ. policy, 89 (2016).
- [26] Handan Gulce, VolkanEskizeybey, Biracan |Haspulat, Fahriye Sari, Ahmet Gulce, Ahmet Avce, ACS, 54 (2013).
- [27] De-En Gu, Bang-Chao Yang, Yong-Da Hu, Catal.Lett.118, 254 (2007).
- [28] Kaori Nishizawa, Masahisa Okada, EijiWatanabe, Materials sciences and Applications5, 112 (2014).
- [29] Liuxue Zhang, Peng Liu, Zhixing Su, Polymer degradation and stability 91,2213 (2006).
- [30] Xu Shoubin, Jiang Long, Yang Haigang, Song Yuanging, Dan Yi, Chinese Jr. of catalysis 32, 4 (2011).
- [31] Matthias Georg Schwab, Manual Hamburger, Jie Shu, Hans Wolfgang Spies, Kinchen Wang, Markus Antonietti, Xinliang Feng, Klaus Mullen, ESI, RSC, 21 (2010).
- [32] Lianwei Li, Ryan Hadt, Shiyu Yao, Wai-Yip Lo, Zhengxu Cai, Qinghe Wu, Bill Pandit, Lin X. Chen, Luping Yu, Chemistry materials ACS, 43 (2010).
- [33] NilakshiSadavarte, C.V.Avadhani, Prakash P.Wadgaonkar, High performance polymers 23(7), 494 (2011).

- [34] Yopendra, Suneel Naik, Mahadevan, Madhusudhana, International Jr. of Environ. Sciences and Research**1**(1), 11 (2011).
- [35] Ali Mahyar, Mohammad Ali Behnajady, Naser Modirshahla, Photochemistry and photobiology**87**, 795 (2011).
- [36] Yong-Gang Peng, Jun-Ling Ji, Yun-Long Zhang, Huai-Xin Wan, Da -Jun Chen, Environ. progress& sustainable energy 30 (2013).
- [37] Sandeep M. Tripathi, Devendra Tiwari, Arabinda Ray, Electrical Indian Jr. of Chemistry**53A**, 1505 (2014).
- [38] Rajeev Arora, Anupam Srivastav, Utam Kumar Mandal, IJMER**2**(4), 2384 (2012).
- [39] Amir Mostafaei, Ashkan Zolriasatein, Progress in natural science: Materials International **22**(4), 273(2012).
- [40] TursunAbdiriyum, Ahmat Ali, Ruxangul Jamal, Yakupjan Osman, Yu Zhang, Nanoscale research letters**9**, 89 (2014).
- [41] Elena Perji, Lidia Ghimpu, Gabriela Hitruc, Valeria Harabagiu, Maria Bruma, Luminita Marin, High performance polymers**27**(5), 546 (2015).